

Study of antiproton annihilation at rest in liquid and gaseous hydrogen into three neutral pseudoscalar mesons

M.Herz (Crystal Barrel Collaboration)
ISKP-University of Bonn, Nussallee 14-16, D-53115 Bonn

All-neutral data have been taken with the Crystal Barrel Detector at LEAR/CERN providing high-statistics data samples of protonium annihilation in gaseous hydrogen at 12 atmospheres. The six-photon final state has been selected in order to yield data sets on $\pi^0\pi^0\pi^0$, $\pi^0\pi^0\eta$ and $\pi^0\eta\eta$ comparable in statistics to data of antiproton annihilation in liquid hydrogen from former run periods. Production of scalar resonances is favoured in liquid hydrogen where annihilation from initial S-state dominates. In gaseous hydrogen a larger amount of initial P-state annihilation contributes to the final states. Data are presented and preliminary results of partial wave analyses and the ratio of S- versus P-state annihilation rates are given.

1 Data

Data of antiproton annihilation both in liquid (LH_2) and in gaseous hydrogen (GH_2) into three neutral pseudoscalar meson final states are presented in the form of Dalitz plots in figure 1. The high statistics data samples were taken with the Crystal Barrel Detector at the Low Energy Antiproton Ring LEAR at CERN. Data contain roughly 700000 $\pi^0\pi^0\pi^0$ -events and roughly 280000 $\pi^0\pi^0\eta$ -events for each case. These data are analysed in parallel with data on the isoscalar $\pi\pi$ -phase shift derived from scattering experiments[1]. The final state $\pi^0\eta\eta$ covers roughly 200000 events of annihilations in liquid hydrogen and 70000 events from gaseous hydrogen. Both data sets were collected with a special trigger enhancing the fraction of recorded events with two η -mesons.

2 Partial Wave Analysis

The three body final state is assumed to be produced according the Isobar Model. The protonium initial state carries the quantum numbers J^{PC} . In a first step a resonance with quantum numbers J^{PC} is produced recoiling against a

meson such that angular momentum is conserved. After propagation the resonance decays into two pseudoscalar mesons. In order to conserve unitarity and time reversal invariance the K -matrix formalism has been chosen where a symmetric and real K -matrix is used to express the scattering part via

$$\hat{T} = (I - 2i\hat{K})^{-1}\hat{K} \quad (1)$$

The process of formation of a resonance of spin l then reads

$$\hat{F}^l = (I - i\hat{K})^{-1}\hat{P} \quad (2)$$

where the production strengths of the given resonance is given by the vector \hat{P} . The overall transition amplitude for protonium annihilation at rest then reads

$$\mathcal{A} = \Sigma Z_{J^{PC}, L, l} \cdot F^l \cdot B^L \quad (3)$$

where Z stands for the coupled angular distribution of the overall process times the dynamical part F^l times a centrifugal barrier factor B^L for the isobar production. Pairs of data then are coupled by scaling parameters of the production strengths in each $\bar{p}p$ -initial state.

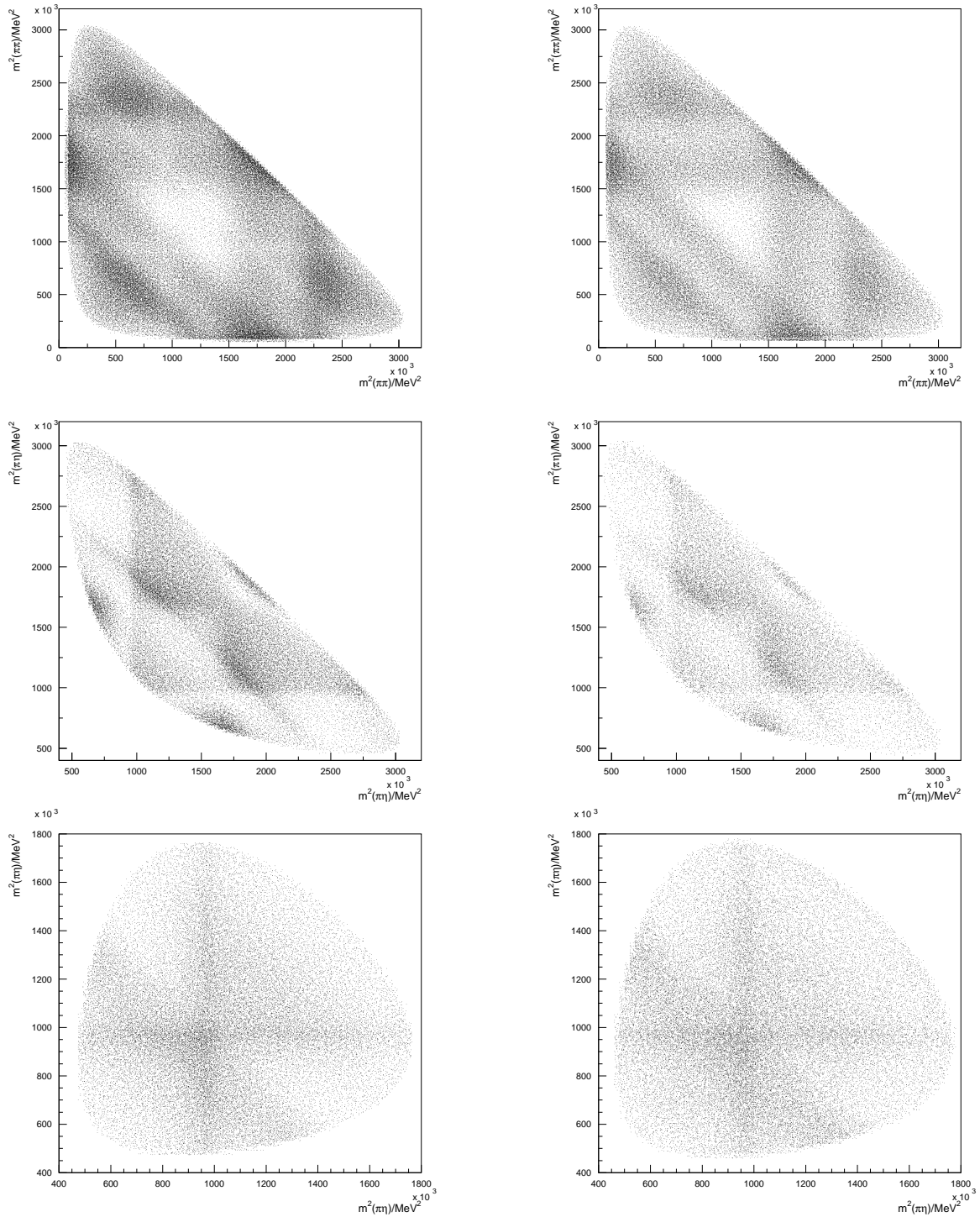


Figure 1: Dalitz Plots for $\bar{p}p$ annihilation at rest into $\pi^0\pi^0\pi^0$ (top), $\pi^0\pi^0\eta$ (center) and $\pi^0\eta\eta$ (bottom) of antiprotons stopping in liquid hydrogen (left) and gaseous hydrogen at 12 atm (right)

3 Protonium Cascade Model

The basic assumptions on the initial protonium state follow the picture that antiprotons entering the target volume moderate by multiple scattering until they stop. The \bar{p} appears to be captured in atomic hydrogen orbits of principle quantum numbers $n \approx 30$ where the Bohr radius of the antiproton is comparable to that one of an electron in the hydrogen ground state. This highly excited $\bar{p}p$ state is formed in ejecting the electron by *Auger effect*. Deexcitation is then possible via dipole radiation which is most likely to happen in vacuum or via external Auger effect in the presence of nearby molecules. Chemical effects like dissociation or rotational and vibrational transitions may contribute as well. The protonium state then experiences strong and fluctuating electrical fields of neighbouring H_2 -molecules. This leads to mixing of angular momentum states due to *Stark Effekt* so that rapid transfers to atomic S- and P-states occur. As soon as the wavefunctions of \bar{p} and p overlap sizeably annihilation takes place. The fraction of S- and P-state annihilation rates depends strongly on the target density. In LH_2 annihilation occurs mostly from high- n initial S-wave orbits. In $GH_2(\rho_{STP})$ S- and P-state contribute equally to the final states; in $GH_2(300\text{ mbar})$ P-state annihilation dominates by $\approx 87\%$. Mixing effects and dynamical effects may alter the population of atomic states compared to their statistical weights so that the final fraction of annihilation rates can be written as

$$F_P = f_P(\rho) \cdot \omega(J^{PC}) \cdot E(J^{PC}, \rho) \quad (4)$$

$$F_S = (1 - f_P(\rho)) \cdot \omega(J^{PC}) \cdot E(J^{PC}, \rho) \quad (5)$$

where f_P is the total P-state annihilation rate, ω is the statistical weight and E is an empirical factor describing suppressed or enhanced populations of each initial state. Branching ratios of two meson final states both in liquid and in gaseous hydrogen have been used to determine fractions[3] given in table 1.

	$^{2S+1}L_J$	LH_2	$GH_2(12\text{ atm})$	<i>ratio</i>
F	1S_0	0.224	0.1442	0.644
	3S_1	0.645	0.4258	0.660
	1P_1	0.0278	0.1038	3.734
	3P_0	0.0277	0.0501	1.809
	3P_1	0.0223	0.0952	4.269
	3P_2	0.0522	0.1808	3.464

Table 1:
Fractions of annihilation rates for each initial state

4 Results

From analyses of the three pseudoscalar meson final states for protonium annihilation into $\pi^0\pi^0\pi^0$, $\pi^0\pi^0\eta$ and $\pi^0\eta\eta$ the Crystal Barrel Collaboration reported the observation of isoscalar and isovector states decaying into two neutral mesons. Apart from already known states like $f_0/a_0(980)$ and $f_2(1270)/a_2(1320)$ the scalar states $f_0(1370)$, $f_0(1500)$ and $a_0(1450)$ have been discovered. Evidence for tensor states like $f_2(1565)$ and $a_2(1650)$ were found but data had partly ambiguous solutions; in particular the S/P ratio was not well defined. Therefore data have been taken in gaseous hydrogen at 12 atmospheres in order to constrain the contributions from S- and P-initial state. The use of different target pressures does influence the dynamics of the $\bar{p}p$ -initial state as can be seen already from differences in corresponding Dalitz plots.

4.1 $\pi^0\pi^0\pi^0$ analysis

In this analysis three scalar resonances were allowed. The amplitude of the $(\pi\pi)_S$ -wave was constrained by the scalar $\pi\pi$ -phase shift and elasticity from scattering experiments[1]. In addition one more state above phase space is introduced in order to give this phase a natural continuation. In the same way two plus one tensor resonances were introduced as $(\pi\pi)_D$ -wave. Coupling of both data sets is achieved by global scaling factors of the production strengths for each initial state that finally extracted T -matrix poles for each wave can be given as in table 2 and table 3.

	Mass	Width
$f_0(980)$	983	80
$f_0(1300)$	1290	370
$f_0(1500)$	1496	128

Table 2: T -matrix poles $(\pi\pi)_S$ -Wave

	Mass	Width
$f_2(1270)$	1270	200
$f_2(1565)$	1540	180

Table 3: T -matrix poles $(\pi\pi)_D$ -Wave

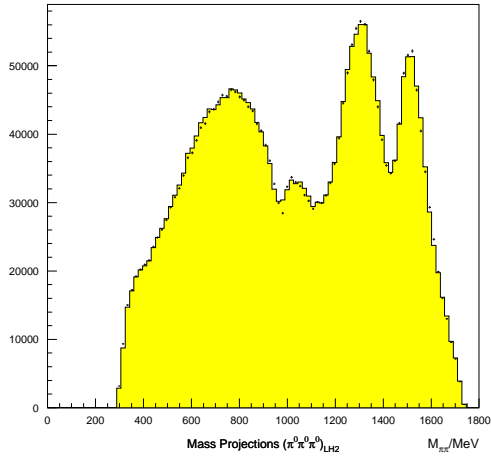


Figure 2: Fits to data on $\bar{p}p \rightarrow \pi^0 \pi^0 \pi^0$

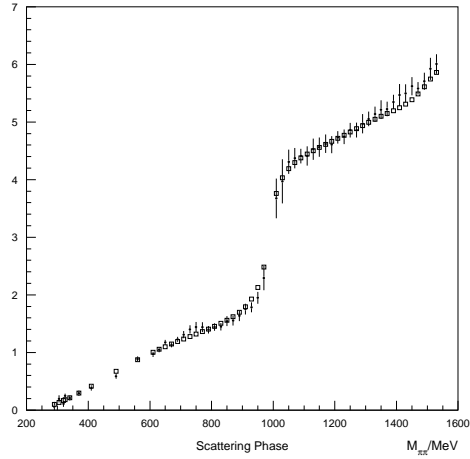
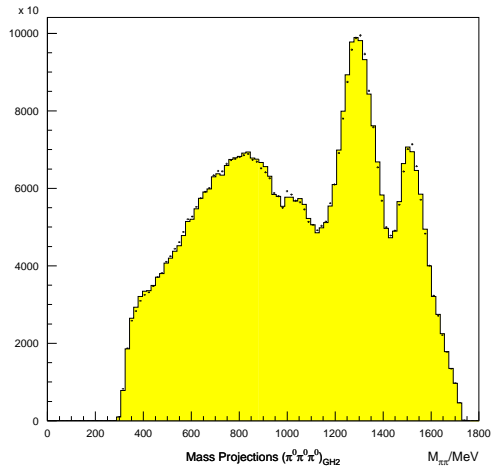


Figure 3: Fits to phase shift and elasticity

Data could be described with $\chi^2_{LH_2} = 1.45$, $\chi^2_{GH_2} = 2.06$ and $\chi^2_{tot} = 1.67$. Phase shift and elasticity have been taken into account with $\chi^2_{SC} = 1.02$. Fits to data are shown in figure 2 and figure 3 as an example in this particular case. The contributions from all three possible initial states are given in table 4.

$^{2S+1}L_J$	LH_2	GH_2	ratio
1S_0	91%	53%	0.5824
3P_1	4%	24%	6.0000
3P_2	5%	23%	4.6000

Table 4: $\pi^0\pi^0\pi^0$ -final state contributions

4.2 $\pi^0\pi^0\eta$ analysis

For the analysis of the $\pi^0\pi^0\eta$ final state we used the solution found for the $(\pi\pi)_S$ -wave as fixed input. The early dropping $\pi\pi$ -phase space in this data of protonium annihilation at rest provides not much information on the following crucial part with respect to $f_0(1300)$. Additionally $f_0(980)$ shows up as clear peak, not as dip as in $\pi^0\pi^0\pi^0$ -data. $f_2(1270)$ is used fixed to describe tensor intensity being expected to contribute in GH_2 data. This time coupling between both data sets for each initial state is imposed by cascade model calculations (table 1) as a check of consistency with the idea behind it. Finally one gets the representations of $(\pi\eta)_{S,D}$ -waves in terms of T -matrix poles (table 5, table 6). Data description

	Mass	Width
$a_0(980)$	978	128
$a_0(1450)$	1496	236

Table 5: T -matrix poles of $(\pi\eta)_S$ -wave

	Mass	Width
$a_2(1320)$	1314	112
$a_2(1650)$	1603	258

Table 6: T -matrix poles of $(\pi\eta)_D$ -wave

can be improved by allowing for one more contribution from an exotic state $\pi_1(1405)$ with quan-

tum numbers $J^{PC} = 1^{-+}$. Its mass and width was found at $M = 1390$ and $\Gamma = 190$. Further studies of this object are presently in progress. Data could be described with $\chi^2 = 1.69$ and $\chi^2 = 1.58$ for LH_2 - and GH_2 -data respectively with contributions from all three possible initial states as given in table 7.

$^{2S+1}L_J$	LH_2	GH_2	ratio
1S_0	90%	61%	0.6777
3P_1	4%	14%	3.5000
3P_2	6%	25%	4.1666

Table 7: $\pi^0\pi^0\eta$ -final state contributions with respect to cascade model predictions

4.3 $\pi^0\eta\eta$ analysis

As pointed out in the beginning GH_2 -data of $\pi^0\eta\eta$ -final state lack in statistics by a factor of three compared to LH_2 -data where a high statistics data set is available. This leads to quite some difficulties in fitting data freely. Especially in the neighbourhood of $f_0(1500)$ and for the higher mass part GH_2 -data tend to smear resonance structures when coupling both data sets. Therefore in order to constrain data description as much as possible again the method of fixed couplings has been applied. Nevertheless in fee-

	Mass	Width
$f_0(1300)$	1387	340
$f_0(1500)$	1520	160
$f_0(1750)$	1690	180

Table 8: T -matrix poles of $(\eta\eta)_S$ -wave

	Mass	Width
$f_2(1565)$	1518	82
$f_2(1810)$	1753	274

Table 9: T -matrix poles of $(\eta\eta)_D$ -wave

ding in $\pi\eta$ -waves of the preceding analysis one yields representations of the $(\eta\eta)_{S,D}$ -waves as given in table 8 and table 9 with $\chi^2_{LH_2} = 1.34$ and

$^{2S+1}L_J$	LH_2	GH_2	ratio
1S_0	89%	56%	0.6292
3P_1	8%	30%	3.7500
3P_2	3%	12%	4.0000

Table 10:
 $\pi^0\eta\eta$ -final state contributions with respect to cascade model predictions

$\chi^2_{GH_2} = 1.26$. $f_0(1500)$ and $f_2(1565)$ appear to mix heavily which is indicated by finding almost equal masses for both resonances. The hadronic width of the scalar resonance seems broader than usual whereas the tensor state shows up rather narrow. Each initial state appears to contribute according table 10.

5 Summary

As shown LH_2 - and $GH_2(12\text{ atm})$ -data of antiproton annihilation at rest can be described simultaneously in accordance to protonium cascade model calculations. In this picture antiprotons are captured in high atomic orbits before they cascade down to low angular momentum states due to electromagnetic interactions.

Then as soon as strong interaction leads to annihilation multiple meson final states occur where the case of three neutral particles has been studied. In liquid hydrogen S-state annihilation occurs to $\approx 90\%$ whereas in gaseous hydrogen to $\approx 55\%$. The remaining intensity in each case is spread over the two possible initial states almost equally according to nearly equal hadronic widths of these states [4]. Isoscalar and isovector states contributing to the final states are given in the appropriate sections in terms of T -matrix poles. Evidence for the hybrid candidate $\pi_1(1405)$ is rather weak and may not exceed few percent even in GH_2 -data where additionally the 3P_1 initial state for its production is contributing more than in LH_2 -data.

References

- [1] G.Grayer et al., Nucl.Phys. B75,189(1974)
- [2] S.U.Chung et al., Ann.Phys. 4,404(1995)
- [3] C.J.Batty, Nucl.Phys. A601,425(1996)
- [4] J.M.Richard,M.E.Sainio,
Phys.Lett. B110,349,(1982)